Objective Indicators of the Life Cycle Evolution of Extratropical Transition for Atlantic Tropical Cyclones

JENNI L. EVANS AND ROBERT E. HART

Department of Meteorology, The Pennsylvania State University, University Park, Pennsylvania

(Manuscript received 28 August 2001, in final form 14 June 2002)

ABSTRACT

Forty-six percent of Atlantic tropical storms undergo a process of extratropical transition (ET) in which the storm evolves from a tropical cyclone to a baroclinic system. In this paper, the structural evolution of a base set of 61 Atlantic tropical cyclones that underwent extratropical transition between 1979 and 1993 is examined. Objective indicators for the onset and completion of transition are empirically determined using National Hurricane Center (NHC) best-track data, ECMWF 1.125° × 1.125° reanalyses, and operational NCEP Aviation Model (AVN) and U.S. Navy Operational Global Atmospheric Prediction System (NOGAPS) numerical analyses. An independent set of storms from 1998 to 2001 are used to provide a preliminary evaluation of the proposed onset and completion diagnostics.

Extratropical transition onset is declared when the storm becomes consistently asymmetric, as measured by the 900–600-hPa thickness asymmetry centered on the storm track. Completion of the ET process is identified using a measure of the thermal wind over the same layer. These diagnostics are consistent with the definitions of tropical and baroclinic cyclones and are readily calculable using operational analyses. Comparisons of these objective measures of ET timing with more detailed three-dimensional analyses and NHC classifications show good agreement.

1. Introduction

No universally accepted definition of extratropical transition of tropical cyclones [(ET)] presently exists (Malmquist 1999) yet, on average, 46% of Atlantic tropical storms (Hart and Evans 2001), 27% of western North Pacific storms (Klein et al. 2000), and 10% of storms in western Australian waters (Foley and Hanstrum 1994) undergo ET. Forecasters must rely on subjective assessments of asymmetry of the storm's cloud shield and its passage over colder water to discern the onset and completion of transition, yet weakening or recurving storms may also exhibit these characteristics (L. Avila 1999, personal communication). In this paper, we propose objective diagnostics to mark both the onset and completion of ET and evaluate these using an independent group of storms. First, we review the existing literature to provide a perspective on likely fruitful choices for diagnostics of extratropically transitioning storm structure.

Tropical storms that undergo ET evolve from systems with compact wind fields and relatively symmetric rainfall patterns to highly asymmetric systems moving at 10 m s^{-1} or more, in which the peak wind speeds are usually much reduced, but the area of gale or storm force winds is often vastly increased (e.g., DiMego and Bosart 1982a,b; Foley and Hanstrum 1994; Harr and Elsberry 2000; Hart and Evans 2002, manuscript submitted to *Mon. Wea. Rev.*, hereafter HAE; Klein et al. 2000; Sekioka 1956a,b; Thorncroft and Jones 2000). The damaging winds and rains in an extratropically transitioned storm are typically on opposite sides of the storms and a heavy rain belt extends over vast regions (e.g., Atallah 2001; Bosart et al. 2001). Additionally, extreme ocean waves generated by ET systems in the North Atlantic provide challenges for Canadian maritime forecasts (Bowyer 2000; MacAfee and Bowyer 2000a,b).

In summary, a storm undergoing ET will exhibit an increasingly asymmetric thermal field in response to its interaction with the baroclinic midlatitude environment and will develop a cold-core structure, traceable through its thermal wind profile. Consequences of these structure changes include intense rainfall and extreme ocean waves, but the storm structure changes described suggest straightforward ET diagnostics based on height/thickness fields. After a brief discussion in section 2 of the data used, expected storm structure changes are reviewed in section 3. The new ET onset/completion diagnostics will be presented and examined in section 4 using a sample of 61 Atlantic storms (1979–93). An independent assessment of these diagnostics is provided

Corresponding author address: Prof. Jenni L. Evans, Dept. of Meteorology, The Pennsylvania State University, 503 Walker Bldg., University Park, PA 16802-5013.
E-mail: evans@essc.psu.edu

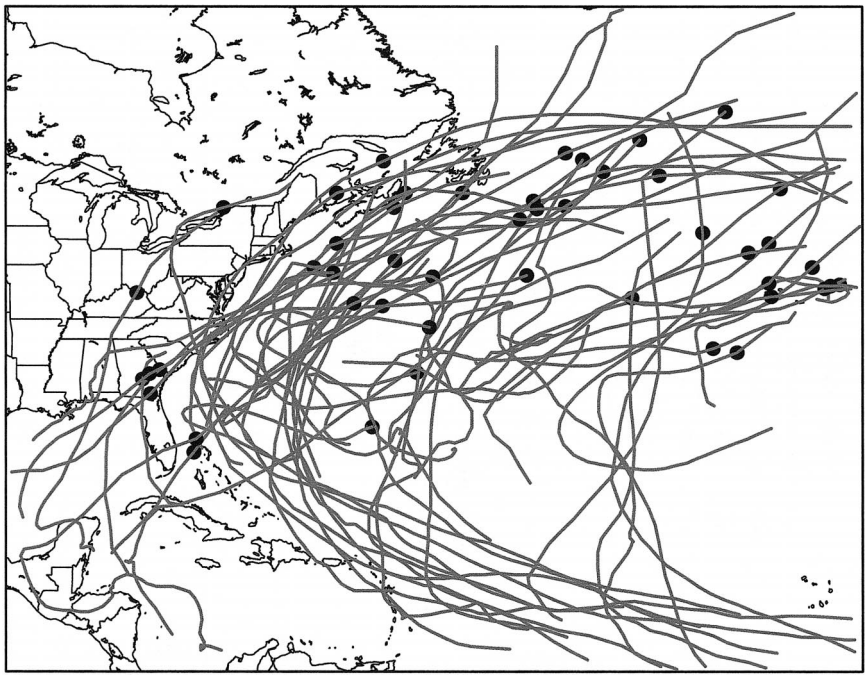

FIG. 1. Tracks of all extratropically transitioning Atlantic tropical storms from the 1990s. The location of transition for each storm, as determined by NHC, is marked with a dot. Note the wide range of latitudes over which ET can occur.

in section 5, where they are tested for several ET cases from the 1998–2001 Atlantic hurricane seasons. Finally, a summary and evaluation of these diagnostics as forecast tools is given in section 6.

2. Data sources and analysis techniques

Sixty-one Atlantic tropical cyclones from the 15-yr period 1979–93 form the dependent dataset for this study; all of these storms had been declared by the National Hurricane Center (NHC) to have undergone ET. Position, intensity, and cyclone stage for these storms, as well as for an independent dataset from the 1998–2001 seasons are obtained from the NHC best-track data.

Figure 1 is a map of the tracks of transitioning Atlantic storms from the 1990s, illustrating the recurving nature of the storm tracks and the wide range of latitudes over which ET occurs.

a. Global datasets (reanalyses and operational)

The European Centre for Medium-Range Weather Forecasts (ECMWF) reanalysis dataset (Gibson et al. 1997) provides numerically consistent analyses of the storms and their environment, free of synthetic (''bogused'') tropical cyclone vortices. The high-resolution analyses used here span the 15-yr period of interest (1979–93) and have 1.125° × 1.125° resolution on 31 vertical levels. This resolution is sufficient to capture the broadscale storm evolution during ET [Hart and Evans (2001), hereafter HE2001]; we used only the 2.5° for HE2001] and for analyses of tropical cyclones (Molinari and Vollaro 1989, 1990). Basin-scale analyses of surface pressure, winds, vorticity, potential vorticity (PV), equivalent potential temperature (θ_E), and other fields provide a fundamental description of the evolving storm structure and environment. Reynolds' weekly averaged sea surface temperature (SST) fields (Reynolds and Smith 1995) provide 1.0° × 1.0° real-time spatial distributions of Atlantic SST for each storm.

Analyses of the independent set of storms from the 1998–2001 seasons were performed using 1° × 1° analyses from both the National Centers for Environmental Prediction (NCEP) Aviation Model (AVN; Kanamitsu 1989) and the U.S. Navy Operational Global Atmospheric Prediction System (NOGAPS; Hogan and Rosmond 1991) operational global models. Hence the operational analyses available for this study have comparable resolution to the ECMWF reanalyses.

b. Definitions used in this paper

The NHC definition of a ''transitioning tropical cyclone,'' or simply ET, refers to a storm that transitions from tropical to extratropical at some point in its lifetime: prior to the NHC transition point, the storm is in its *tropical phase* (TC), after the storm becomes more asymmetric (based on the satellite signature) NHC declares transition and the storm is in its *extratropical*

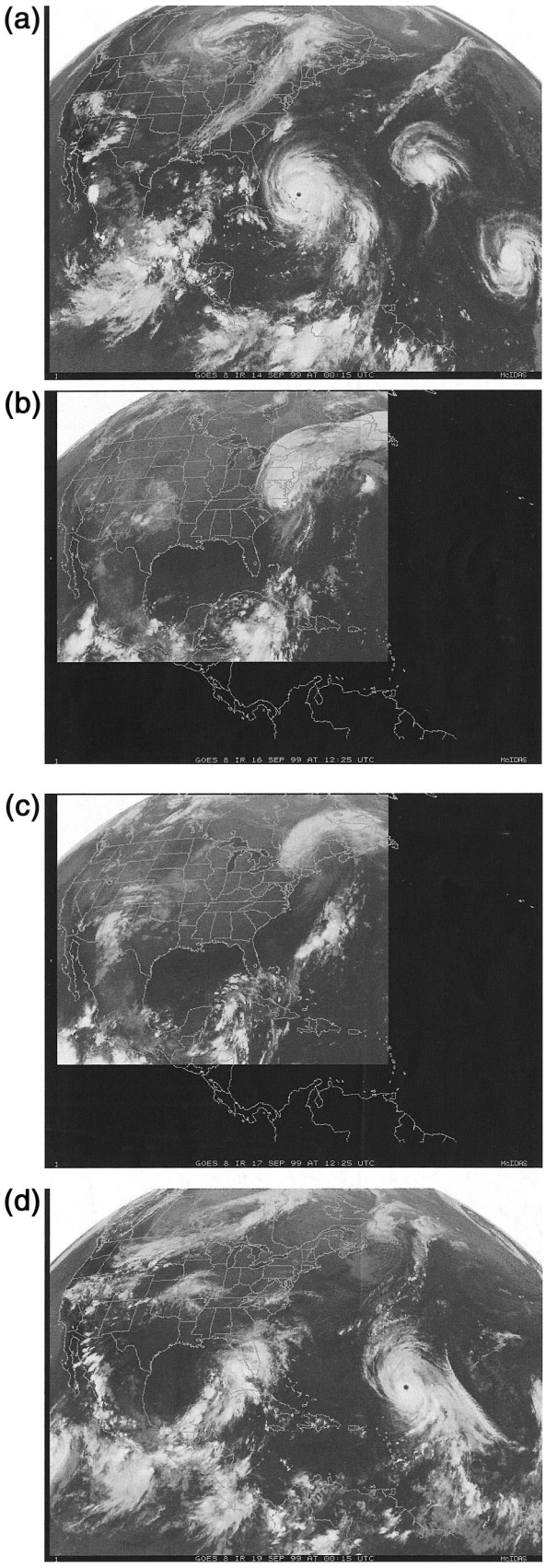

phase (ET). In this study, the *onset* of extratropical transition is defined when the storm asymmetry increases above an empirically determined threshold; *completion* of extratropical transition is defined based on the thermal wind.

3. Storm structural changes expected during ET

The seasonal and synoptic contexts for North Atlantic ET are briefly summarized here and contrasted with the situations in other basins. The evolution of the storm structure through ET described here provides inspiration for the objective ET onset and completion diagnostics proposed in section 4.

a. Seasonality and typical synoptic setup

Atlantic tropical storms that undergo extratropical transition occur predominantly in the months August–October. At least two-thirds of transitioning storms form east of the Caribbean Islands, many as far as the Cape Verde Islands, and recurve ahead of a midlatitude trough into the westerlies (HE2001). Storms forming in the Gulf of Mexico cross the southeast United States, emerging over the Gulf Stream to be swept up into the westerlies (HE2001). Horizontal and vertical wind shears experienced by the storm in the midlatitude baroclinic zone are strong compared to the tropical environment. Midlatitude SSTs are significantly cooler than 26°C, although many ET storms track along the edge of the North Atlantic current until after ET is completed, remaining over relatively warm SST for the typical ET latitudes north of 45°–50°N in the North Atlantic. The longest-lived storms prior to recurvature (in their ''tropical phase'') are the most likely to survive recurvature, transitioning and even reintensifying at high latitudes (HE2001). The case of Hurricane Floyd (1999) at the time it was declared ET by NHC (Pasch et al. 1999) is presented in Fig. 2 (see also section 5a). A significant trough is upstream of the major hurricane (Figs. 2a and 3a), which will eventually introduce a thermal gradient across a cyclone that is initially devoid of significant horizontal thermal gradients. This sudden increase in thermal gradient across the tropical cyclone (and the associated wind shear) is often the first sign of the loss of tropical characteristics and the start of extratropical transition. This is further supported by the wind asymmetries documented in such transitioning systems (e.g., DiMego and Bosart 1982a,b; Thorncroft and Jones 2000).

←

FIG. 2. Hurricane Floyd (1999) *GOES-8* infrared satellite imagery: (a) 0015 UTC 14 Sep (b) 1225 UTC 16 Sep, (c) 1225 UTC 17 Sep, and (d) 0015 UTC 19 Sep.

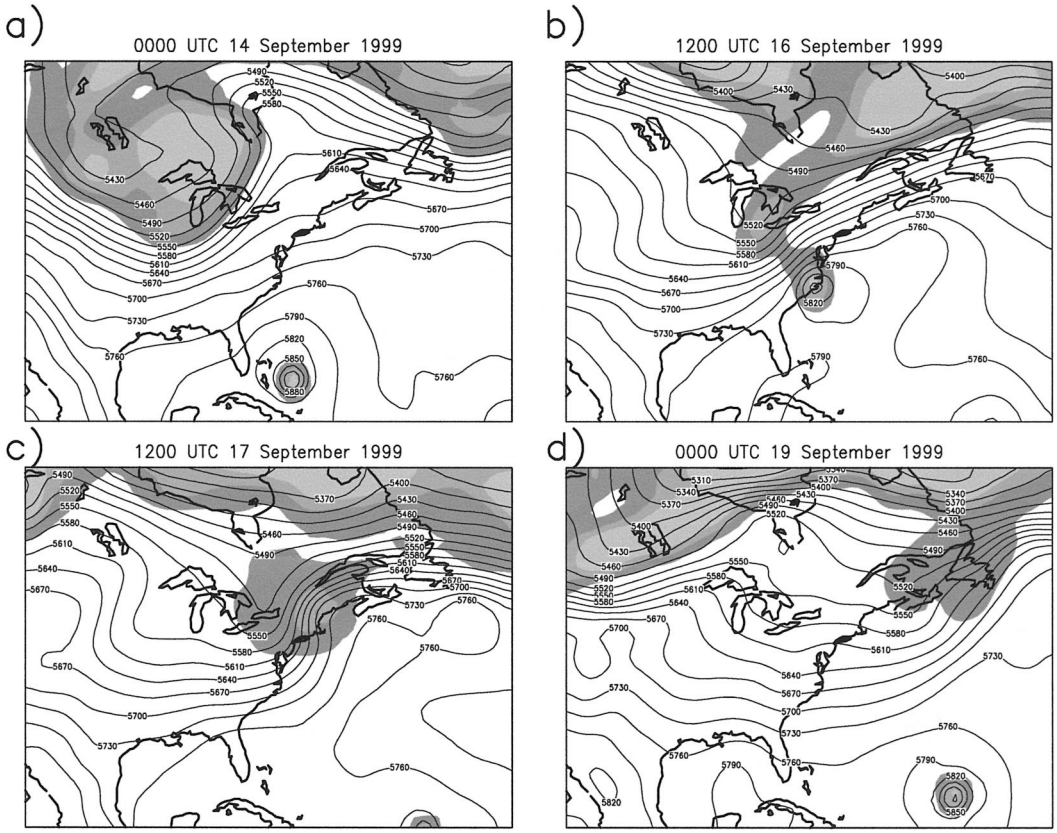

FIG. 3. Hurricane Floyd (1999): 325-K isentropic PV (shaded at 1, 2, and 3 PVU) and 1000–5000-hPa thickness (contoured every 30 m) at (a) 0000 UTC 14 Sep, (b) 1200 UTC 16 Sep, (c) 1200 UTC 17 Sep, and (d) 0000 UTC 19 Sep. Analyses are from NOGAPS 1° × 1° initialization fields.

b. Storm system evolution

A tropical cyclone is defined as a nonfrontal, warm-cored cyclone with origins in the Tropics (Elsberry 1995). Such a definition implies a relatively symmetric steady-state tropical cyclone in gradient wind balance. As a storm proceeds out of the Tropics, its changing environment induces major structural changes in the storm. The low-level shear and strong convergence associated with a tropical cyclone advancing into the midlatitudes concentrates the lower-tropospheric temperature gradients locally, leading to a sharp contrast between the warm, tropical air mass and the cooler, midlatitude air. This sharpening contrast between mean warm and cool background environments may lead to either the destruction or extratropical transition of the tropical cyclone moving into the region. Snapshots of the synoptic situation of the transitioning Hurricane Floyd (1999) at ET onset and completion are plotted in Fig. 3: in Fig. 3b a midlatitude trough (PV $\geq$ 1 PVU $= 10^{-6}$ m^2 K s^{-1} kg^{-1}) is evident approaching the symmetric Floyd; the transitioned storm in Fig. 3c is larger and more asymmetric than its tropical seed. These system changes are briefly reviewed here.

1) ONSET

As a storm commences ET (i.e., begins to take on nontropical characteristics) it becomes decreasingly symmetric. Analyses of the set of 61 Atlantic storms used here reveal that this decrease in symmetry results from the low-level frontogenesis described above. This is in agreement with the diagnostics of Harr and Elsberry (2000) and Klein et al. (2000) who describe low-level frontogenesis as an indicator of ET for western North Pacific systems; Foley and Hanstrum (1994) also describe interaction with a midlatitude trough and subsequent frontogenesis as key stages in the evolution of the western Australian ET cases they document. This increasing asymmetry is key in detecting the onset of transition, but is not unique to transitioning systems, so further evidence of the progression of ET is necessary before the storm is classified as ''transitioned.'' Many tropical cyclones may start extratropical transition, but never complete the process into a fully cold-core cyclone.

2) EVOLUTION AND ET COMPLETION

After the lower-tropospheric wind and thermal field asymmetries become evident in the storm, the system

must continue to evolve midlatitude storm characteristics, or it will not be considered to have completed ET. As such, declaration of the ''time of ET'' for a given storm requires a completion measure as well. In order for a tropical storm to complete ET, it must develop midlatitude storm characteristics, in particular the development of a cold-core thermal wind structure (geostrophic wind speed increasing with height). This characterization of ET completion differs from Klein et al.'s (2000) definition for western North Pacific storms in that it does not require that the storm reintensify (in terms of pressure). While the majority of ET cases in the Atlantic do reintensify after ET begins (HE2001), in agreement with the traditional approach used NHC, we do not require a storm to reintensify in order to classify it as having undergone ET. Further, the rapidly evolving background pressure field (Hart 1999) during extratropical transition may indicate that a cyclone is intensifying despite the slowly rising minimum MSLP. Thus we rely on fundamental structural change to indicate transition, not necessarily intensity change.

4. Diagnostics suggested from ET life cycle

Development of an objective definition of extratropical transition has the potential to be a useful forecast tool and to ensure consistency across regions of responsibility. Hence, guided by the storm structural evolution outlined in section 3, objective diagnostics for the characterization of ET onset and completion are proposed here and empirically defined threshold values for these are explained.

a. Defining ET bounds

Transitioning tropical storms, decaying storms, or storms undergoing transient interactions with other systems may all become asymmetric. Indeed, both transitioning and decaying tropical storms will exhibit a weakening warm-core signature; however, a tropical storm that has completed ET must, by definition, have structure akin to a midlatitude storm. Thus, ET completion must be distinguished by an unambiguous characteristic of midlatitude storms. From hydrostatic implications, changes in the warm-core strength at all levels impact the height field in the lower troposphere (Hirschberg and Fritsch 1993). While the warm-core aloft may weaken or disappear, a thermal wind measure of structure will still indicate an overall warm-core structure in the lower troposphere if the thermal anomaly in the midtroposphere remains warm core. Thus, by focusing on the thermal wind in the lower troposphere, we apply a more stringent criterion on transition completion than by focusing on the upper-troposphere thermal wind. From a thermal wind perspective, the upper troposphere usually becomes cold core prior to the lower troposphere. The lower troposphere is defined here as the 900–600-hPa layer. Finally, these diagnostics will be most readily applied to model output and so must be amenable to use of gridded data using predefined atmospheric layers and must be readily calculable.

The practicality of the ET diagnostics proposed below is demonstrated, first on the dataset of 61 storms from which they were defined and then (in section 5) on an independent set of storms from the 2000 and 2001 seasons.

b. Definition of transition onset

The definition of a tropical cyclone as a nonfrontal, warm-cored cyclone with origins in the Tropics (Elsberry 1995) implies a relatively symmetric steady-state vortex in gradient wind balance. Indeed, when the thickness field around a tropical storm is examined, it is found to be close to circular symmetry even in an evolving system (Fig. 4a; see below). Decreasing symmetry is a key indicator that ET may have begun. As the tropical storm approaches the midlatitude baroclinic zone, low-level frontogenesis sets up in response to the increasing SST gradients and interactions with midlatitude weather features. For a transitioning Atlantic tropical cyclone moving into the westerlies, cooler environmental air will be to its left (north) and warmer, tropical air will be to its right (south), and the low-level frontogenesis described above can be characterized as a shift to a sustained asymmetry in the thickness field in the region of the storm. Hence, *a natural indicator of storm symmetry (for any tropical or extratropical system) is the storm-relative right minus left asymmetry in the thickness field:*

$$B = h[(\overline{Z_{600} - Z_{900}})_R - (\overline{Z_{600} - Z_{900}})_L], \qquad (1)$$

where the overbar indicates the areal mean over the semicircle with respect to storm motion and h indicates the hemisphere [1 = Northern Hemisphere (NH), −1 = Southern Hemisphere (SH)]. However, a horizontal scale over which to measure this asymmetry must be determined.

An appropriate radius for B would be one that includes the convergent circulation of the tropical cyclone, but does not extend into other systems that are not yet influencing the tropical cyclone. Accordingly, the radius for B was chosen to be consistent with the average radius over which cyclonic, convergent inflow was observed for tropical cyclones: 4°–6° (Frank 1977a). Inspection of the PV fields in Fig. 3 reveals that the storm signature is confined well inside 500-km radius in both tropical and extratropical phases. Exploration of the complete dependent dataset of 61 storms and dozens of midlatitude systems confirms that the 500-km radius is a reasonable horizontal area to use to describe the storm/environment evolution (Hart 2003, hereafter HAR). *The ET onset is defined according to*

$$B > 10 \text{ m},$$

where the 10-m threshold is justified below.

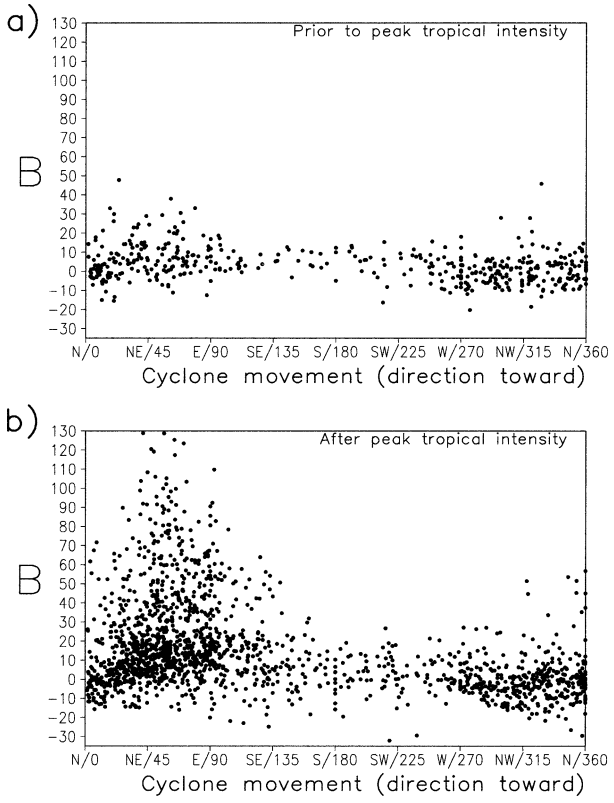

FIG. 4. Scatterplot of storm motion direction (toward) and ET onset diagnostic, *B*, for (a) tropical storms prior to their peak intensity and (b) storms after their peak tropical intensity. Storms moving toward the north through northeast (i.e., during and after recurvature) have the highest degree of asymmetry (larger values of *B*) and variability.

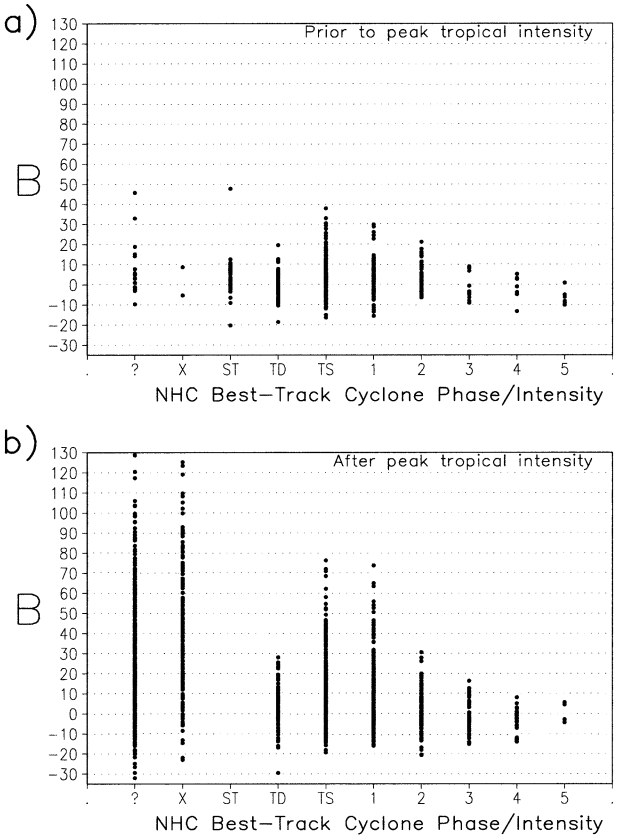

FIG. 5. Distribution of cyclone phase/intensity vs *B* for (a) tropical storms prior to their peak intensity and (b) storms after their peak tropical intensity. The 10-m threshold for distinguishing tropical environments from marginal frontal environments is illustrated well by the distribution for category 3 and greater hurricanes as compared to other cyclone types and intensities. The *x* axis represents cyclone phase and intensity: *x* = extratropical, TD = tropical depression, TS = tropical storm, 1–5 Saffir–Simpson hurricane scale. The question mark indicates that no best-track data were available for the cyclone.

Scatterplots of storm heading (movement toward) versus *B* (the 900–600-hPa thickness asymmetry) for the 61-storm dependent sample are presented in Fig. 4 for storms (a) prior to peak tropical intensity and (b) after peak tropical intensity, as recorded in the NHC best tracks. As expected, this measure of storm structure indicates a generally high degree of symmetry with little variability for purely tropical storms (Fig. 4a). For perfect symmetry $B = 0$, however, both small-scale transient storm asymmetries, cyclone tracking uncertainties, and data analysis uncertainties require that this threshold be relaxed. Comparison of Figs. 4 and 5 provides justification for an *empirically determined threshold of B* $= 10$ m to distinguish between purely tropical storms (which rarely exceed this threshold; Fig. 4a, TCs of category 3 and above on the Saffir–Simpson hurricane scale). The few ''tropical phase'' cases in which $B < -10$ m (implying a warm poleward and cold equatorward asymmetry) are weak tropical storms that are likely not well resolved by the analyses or where the tracking was slightly off.

This $B > 10$ m symmetry diagnostic has proven to be very robust. This diagnostic failed in only one weak, open-ocean case (Tropical Storm Allison 1989) out of 41 cases in 10 yr. A check on the statistical significance of the differences between the two storm samples represented in Figs. 3a and 3b (Student's *t* test) reveals that the mean and median *B* values for the two samples are significantly different to 99% confidence for all cyclone phases except category 3–5 hurricanes.

c. Detection of transition completion

An unambiguous and distinguishing characteristics of a midlatitude storm is its cold-cored structure, so we define ET completion as thermal wind corresponding to a cold-cored thermal wind field. The determination of cold-versus warm-core vertical structure is the distinction of whether the magnitude of the cyclone isobaric height gradient ($Z_{MAX} - Z_{MIN}$ within a 500-km radius of the surface cyclone center, proportional to the geostrophic wind magnitude) increases (cold core) or decreases (warm core) with height (Fig. 6). This fundamental difference of thermal wind structure between tropical and extratropical cyclones was exploited to di-

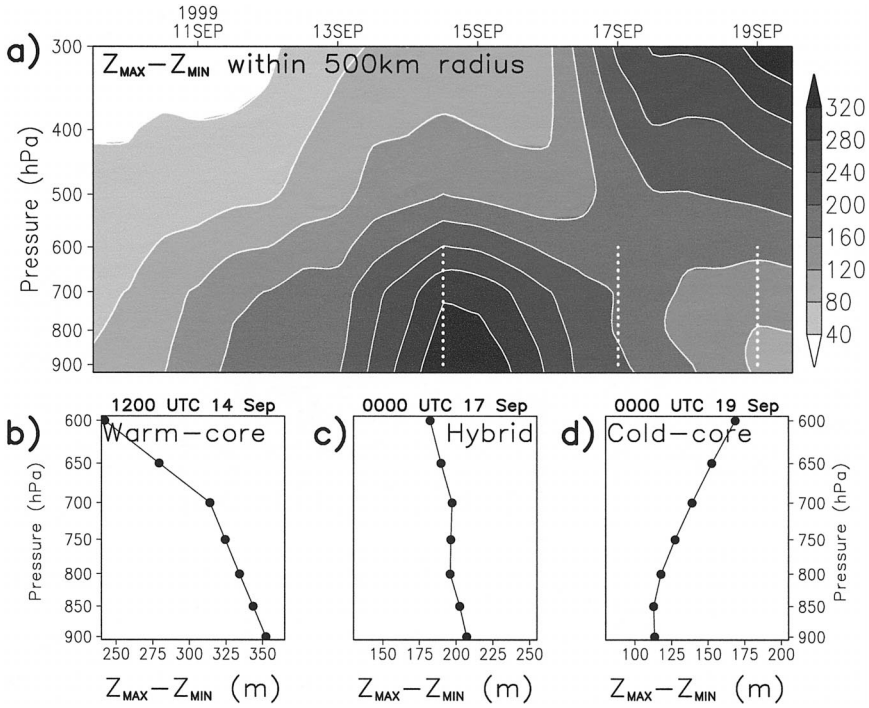

FIG. 6. The warm-to-cold-core evolution during the extratropical transition of Hurricane Floyd (1999). (a) Time–height cross section of Z_{MAX}–Z_{MIN} (m) as interpreted by the 1° × 1° NOGAPS analyses. Vertical profiles of Z_{MAX}–Z_{MIN} between 600 and 900 hPa at three times are given for (b) tropical phase at 1200 UTC 14 Sep, (c) hybrid phase nearing transition completion at 0000 UTC 17 Sep, and (d) extratropical phase at 0000 UTC 19 Sep.

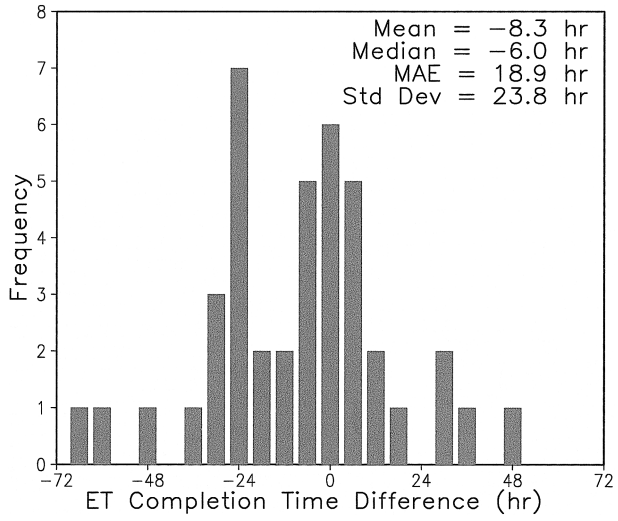

FIG. 7. Comparison of NHC best-track transition times with the timing of the $-|\mathbf{V}_T^L|$ diagnostic of transition completion proposed here for 38 transitioning cyclones between 1979 and 1993. Although the spread of timing difference extends from −72 to +48 h, the majority of cases (20/38) agree within ±6 h.

agnose the cold-versus warm-core cyclone evolution and, ultimately, ET completion. The thermal wind measure of cyclone structure is thus

$$\left.\frac{\partial(Z_{\mathrm{MAX}} - Z_{\mathrm{MIN}})}{\partial \ln p}\right|_{900\ \mathrm{hPa}}^{600\ \mathrm{hPa}} = -\mathbf{V}_T^L. \qquad (2)$$

A warm-cored system will have $-\mathbf{V}_T^L > 0$, implying a larger perturbation at 900 hPa compared with 600 hPa, a positive value of the thermal wind, and a stronger near-surface wind (Fig. 6b). Hence, completion of extratropical transition is indicated when $\mathbf{V}_T^L$ first becomes negative (soon after Fig. 6c).

While the sample of 61 storms studied here were all classified by NHC as having undergone extratropical transition, many storms that begin transition decay before becoming a truly extratropical system, so this diagnostic inevitably shows more variability than the onset measure, yet it still provides useful guidance and consistency with NHC best tracks for over 60% of the 61 cases tested. This is demonstrated in Fig. 7, in which the ET completion times based on this diagnostic are compared to the ET times declared by NHC; negative values indicate that the objective timing leads the NHC declaration. There is good agreement (transition timing within ±6 h) in just over 50% of the cases, with the timings differing by more than 48 h for only two storms

(Fig. 7). The mean time difference for objective declaration of transition compared to the NHC best tracks is −8.3 h, indicating that the objective timing is somewhat earlier than the NHC.

d. Summary of objective diagnostics for ET onset and completion

Based on the diagnostics outlined above, we can objectively define extratropical transition onset and completion as follows:

- *onset of extratropical transition* is marked by sustained thickness asymmetry of >10 m between 900 and 600 hPa;
- this transition onset corresponds to low-level frontogenesis (e.g., Harr and Elsberry 2000);
- *transition is completed* when vertical storm structure corresponds to a cold-cored vortex ($-|\mathbf{V}_T^L| < 0$ implying positive thermal wind) reflecting maximum winds aloft;
- by using the geostrophic wind magnitude profile between 900 and 600 hPa over the storm for the completion diagnostic, both extratropical transition timing diagnostics can be calculated from the height field; and
- the changes in the symmetry and thermal wind shear are measured over a radius of 500 km centered on the storm, rather than at a point, consistent with the extent of the cyclone vortex system diagnosed by Frank (1977a,b).

Using the lower-tropospheric thickness asymmetry and sign of the wind shear to define onset and completion of transition, the mean length of the transition period is found to be just under 1.5 days (Fig. 8). A distinct subset of six cases (of the 61 storms) transitioned over open ocean in the absence of strong trough interaction and could be tracked through 4 or more days before completing transition (Fig. 8). With these cases removed, the mean and median transition times are reduced to 18.4 and 12 h, respectively.

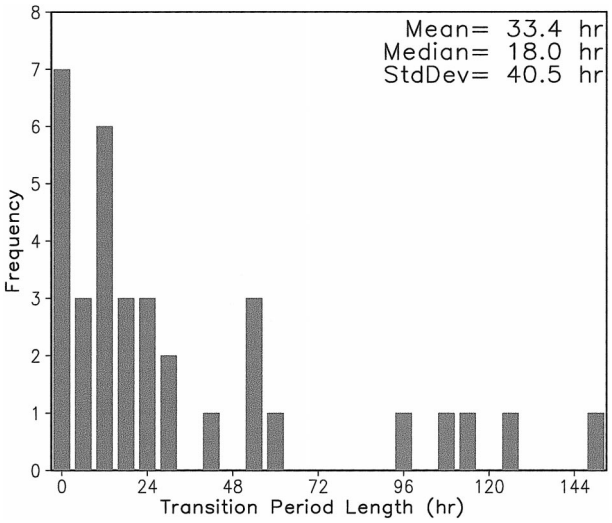

FIG. 8. Frequency distribution of extratropical transition period length, i.e., the time elapsed after $B = 10$ m until $-|\mathbf{V}_T^L| < 0$. This figure represents the 34 of 61 transitioning cyclones available within the 1979–93 period of ECMWF reanalyses that had unambiguous detectable signals in both diagnostics, which allowed calculation of the transition period length.

5. Mapping the transition life cycle

As shown in HAR, the diagnostics above (parameters B and $-|\mathbf{V}_T^L|$) define a cyclone phase space (example given in Fig. 9). The full life cycle of a cyclone is defined through the trajectory through the phase diagram, with time moving forward as one moves along the trajectory, from the labels A–Z. Here, A and Z are not necessarily the formation and decay locations of the storm, but represent the start and end of the cyclone life cycle resolvable within the available dataset and its geographic boundaries. The shading of the markers corresponds to the intensity of the cyclone (minimum central pressure in hPa): the weakest storms (>1010 hPa) are white, and solid black are the most intense (<970 hPa). The size of the cyclone (taken as the mean radius of the 925 hPa gale force wind field area) is represented by the size of the solid circle marker along the phase trajectory (largest shown in Fig. 9 is approximately 600 km). The track of the cyclone is plotted in the inset, with the date marked at the 0000 UTC positions.

a. Graphical summary of storm evolution through ET

The evolution of Hurricane Floyd (1999) from intense tropical cyclone into an extratropical cyclone is shown here through phase analysis (Fig. 9) as a typical example of extratropical transition. The life cycle of Floyd in Fig. 9 begins on 9 September, 1 day after tropical cyclogenesis (Lawrence et al. 2001). Through 15 September, Floyd undergoes classic symmetric warm-core development, and at peak tropical intensity on 15 September 1999. Evaluation of the objective ET diagnostics using the 1° resolution AVN and NOGAPS analyses around this time show Floyd with ($B \approx 0$, $-|\mathbf{V}_T^L| \approx +125$) (Fig. 9a) and ($B \approx 0$, $-|\mathbf{V}_T^L| \approx +250$) (Fig. 9b), respectively. That is, both operational global models are resolving a symmetric cyclone with a strong warm-core signature.

A strong trough approaches the landfalling cyclone over North Carolina on 16 September (Figs. 2 and 3), and Floyd begins its evolution to an extratropical cyclone. This initiation is marked as B first exceeds 10 m, early on 16 September. During 16 September the cyclone has become a frontal warm-core cyclone (hybrid), having characteristics of both tropical and extratropical cyclones that are apparent in satellite imagery animations (Fig. 2). At 1200 UTC 17 September, $-|\mathbf{V}_T^L|$ first

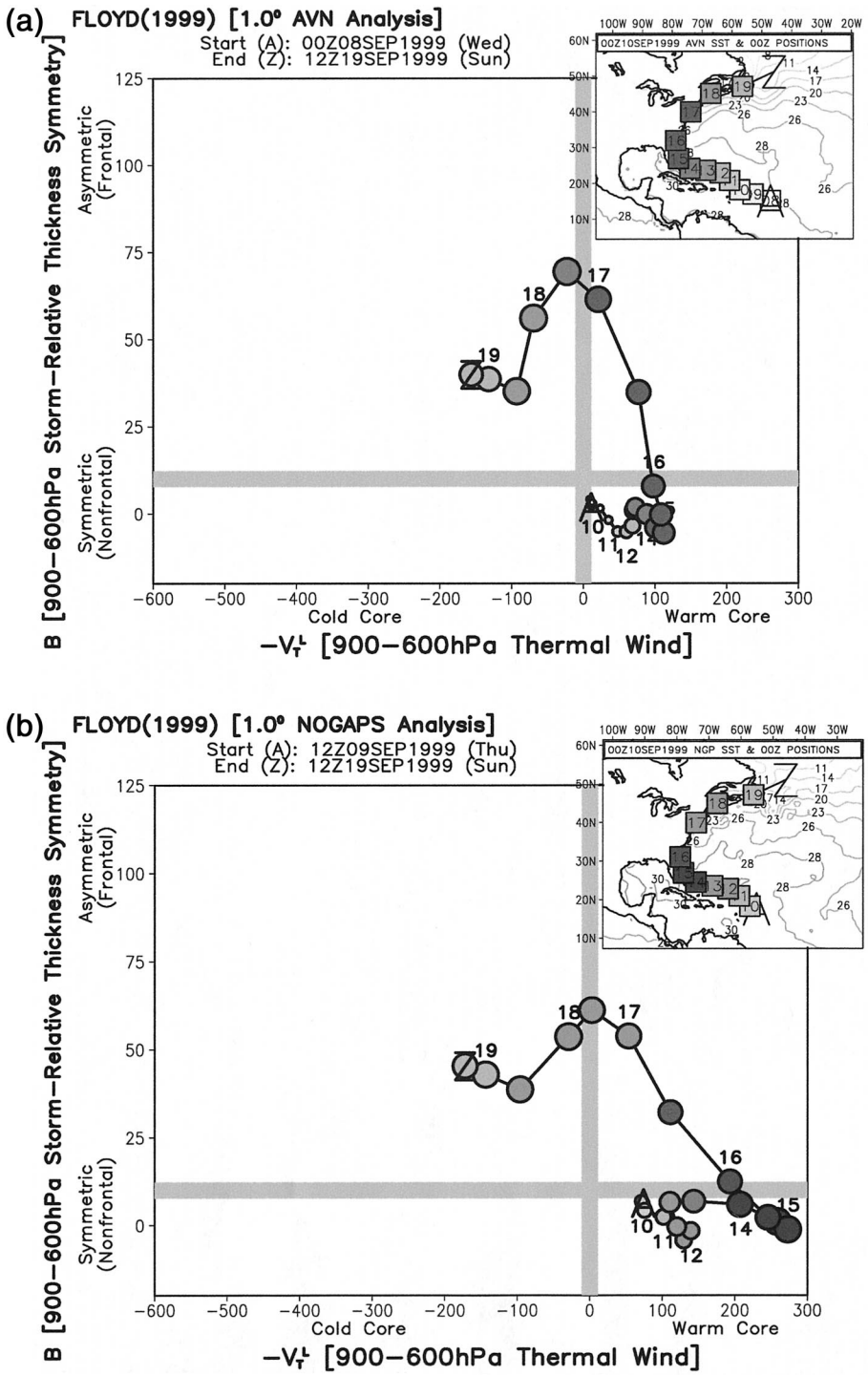

FIG. 9. Hurricane Floyd (1999) ET as represented within cyclone phase space: (a) 1° AVN analyses and (b) 1° NOGAPS analyses. The ordinate indicates the storm symmetry (B) while the abscissa is a measure of the cold-/warm-core structure of the system (rhs of diagram corresponds to $-|\mathbf{V}_T^L| > 0$ for warm core). Time moves forward from A and Z, the start and end of the cyclone life cycle resolvable within the available dataset and its geographic boundaries. The size of the cyclone (mean radius of the 925-hPa gale force wind region) corresponds to the size of the solid circles along the phase trajectory (largest shown is approximately 600 km). Circle shading corresponds to the intensity of the cyclone, with white for the weakest storms (>1010 hPa) and solid black for the most intense (<970 hPa). The track of the cyclone is plotted in the inset, with the date marked at the 0000 UTC positions.

becomes negative (Figs. 6 and 9), indicating that Floyd has acquired a cold-core structure, completing extratropical transition just prior to landfall in Canada at around 1600 UTC. This timing is identical to the official NHC declaration of extratropical transition given in the tropical cyclone best-track dataset (available online at http://www.nhc.noaa.gov/1999floyd.html). Thereafter, the cyclone intensifies its thermally asymmetric, cold-core structure through 20 September (Fig. 9), ultimately merging with another preexisting extratropical cyclone beyond 20 September (not shown).

Floyd (1999) represents a case where extratropical transition occurs relatively quickly, with a hybrid cyclone phase (frontal warm core; upper-right quadrant in Fig. 9) of approximately 24 h, compared to the mean transition period of 33.4 h identified in Fig. 8.

b. Analyses of a sample of storms from the 1998–2001 seasons and Australia

The objective diagnostics of extratropical transition onset ($B > 10$) and completion ($-|\mathbf{V}_T^L| < 0$) described above were developed on a subjective dataset of 61 storm cases from the period 1979–93 using the ECMWF 1.125° reanalysis data. To demonstrate the wider applicability of these cases, an independent set of 16 Atlantic tropical cyclones from 1998 through 2001 is examined here using 1° AVN and NOGAPS operational analyses. The NOGAPS analyses include a tropical cyclone bogus in all 4 yr. The AVN included a bogus during 1998–2000, but not in 2001. Diagnosis of the warm-core phase of Erin (2001) illustrates that, while the presence of a cyclone bogus in the numerical model initial conditions usually produces a stronger warm-core signal, it is not always the case: the AVN does not include a bogus (Fig. 10a), yet the analyses of Erin are stronger in the AVN than the NOGAPS analyses (Fig. 10b) during the tropical phase of Erin (2001).

Four representative trajectories of extratropical transition within the cyclone phase space are shown in Figs. 9–12. Hurricanes Floyd (1999; section 5a and Fig. 9) and Erin (2001; Fig. 10) are representative cases of the path to extratropical transition exhibited by intense tropical cyclones: both storms develop a strong warm core before the transition process begins, exist as a strong hybrid cyclone for at least a day, and then intensify slightly after transition completion. However, while this is arguably the best-documented path to transition, it does not apply to the majority of the transition cases. Such a trajectory requires fortuitous timing: the development of a strong warm core that recurves ahead of an amplifying trough, the relative trough and tropical storm locations must be such that constructive interaction between the two systems can produce extratropical transition before the shear inherent in this environment destroys the tropical cyclone, and the strong warm-core signature enhances the baroclinicity in the extratropical redevelopment phase of the storm evolution (HAE).

Gordon (2000; Fig. 11) represents a case of extratropical transition where landfall has limited the warm-core intensification of the tropical system prior to the start of extratropical transition. Although the cyclone eventually recurves and interacts constructively with a midlatitude trough, the limited warm-core strength limits the degree of potential baroclinic development. As a result, extratropical transition occurs rapidly, and Gordon exists as a hybrid cyclone for less than a day. After extratropical transition, the cyclone quickly occludes and weakens since the atmospheric conditions introduced to the trough by the weak TC are not sufficient for significant baroclinic development.

The final Atlantic case of Gabrielle (2001; Fig. 12) illustrates the most complex type of extratropical transition. This is a case in which a tropical cyclone interacts with a trough while moving along the northern wall of the Gulf Stream. The result is a dramatic competition of forcing: the trough is driving cold-core development of the cyclone, while the Gulf Stream, through surface fluxes, evaporation, and latent heat release, is modulating the cold-core development. Hence, the trough and the strong gradient of SST are simultaneously producing forcings on the cyclone that dramatically increase its degree of asymmetry. The result is a tropical cyclone that exists as a hybrid cyclone for an extended period of time. Indeed, in the case of Gabrielle, the storm exists as a hybrid cyclone for the majority of its lifetime (Fig. 12). As illustrated by the NOGAPS analysis (Fig. 12b), the maximum asymmetry associated with Gabrielle occurs on 20 September, when the cyclone is still warm core. Although the AVN analysis (Fig. 12a) has a less intense hybrid signal, the trajectory is qualitatively quite similar. On 21 September Gabrielle moves north of the Gulf Stream and the trough interaction dominates the evolution, leading to extratropical transition completion and occlusion. This trajectory of extratropical transition often produces cyclones that are the most difficult to forecast since the dramatic interaction between atmospheric and oceanic forcing is difficult to simulate within numerical models.

While the diagnosis of extratropical transition completion for Gabrielle (2001) differs by 2 days between the AVN and NOGAPS analyses shown in Fig. 12, it is for cyclones such as this that the phase diagram diagnostics can provide additional insight over conventional analyses into the model-forecast cyclone evolution. For example, AVN analyses of potential vorticity, equivalent potential temperature, and sea level pressure for 19 September (Fig. 13) and 21 September (Fig. 14), do not provide a consistent picture of the phase (tropical, extratropical, or hybrid) of Gabrielle. This lack of a consistent picture is also true of the NOGAPS analyses (not shown).

Finally, to demonstrate that these analyses are not basin specific, we include the analysis of severe Tropical

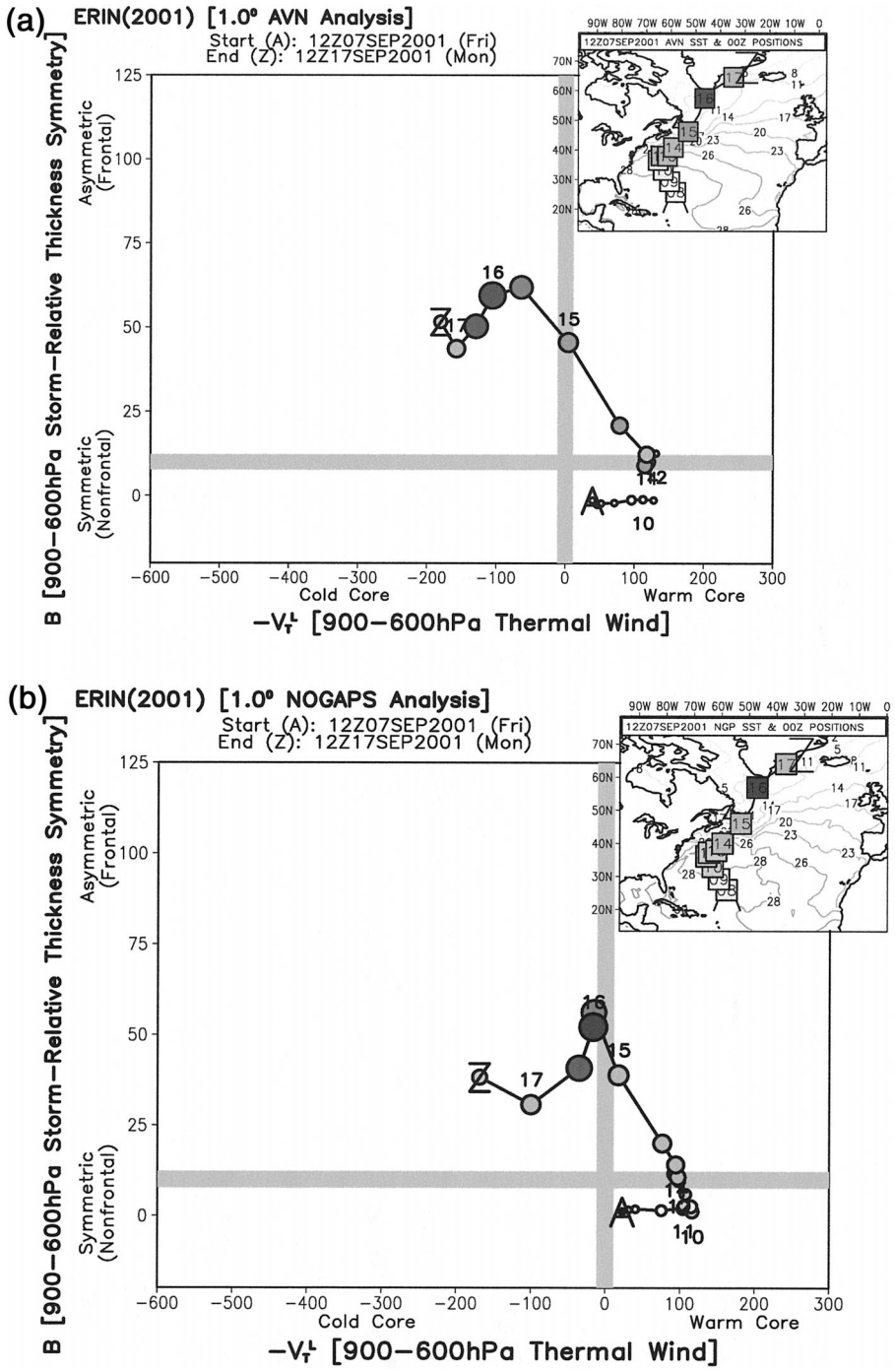

FIG. 10. Phase space diagnostic for Hurricane Erin (2001) using (a) 1° AVN analyses and (b) 1° NOGAPS analyses. Symbols are as in Fig. 9.

Cyclone Vance (1999) from the Australian region. Vance formed in the Coral Sea to the northeast of Australia and tracked along the northern coast to the South Indian Ocean as it gradually intensified. By 1200 UTC 16 March 1999, Vance was just to the west of the Top End over SSTs around 30°C. Over the next 5 days, Vance continued to intensify, becoming a category 5 tropical cyclone at about 1600 UTC on 20 March. Vance's track largely paralleled the coast, until it took a sharp turn at about 1200 UTC on 22 March, coming inland north of Shark Bay (Fig. 15; see inset). Severe Tropical Cyclone Vance had the highest recorded wind

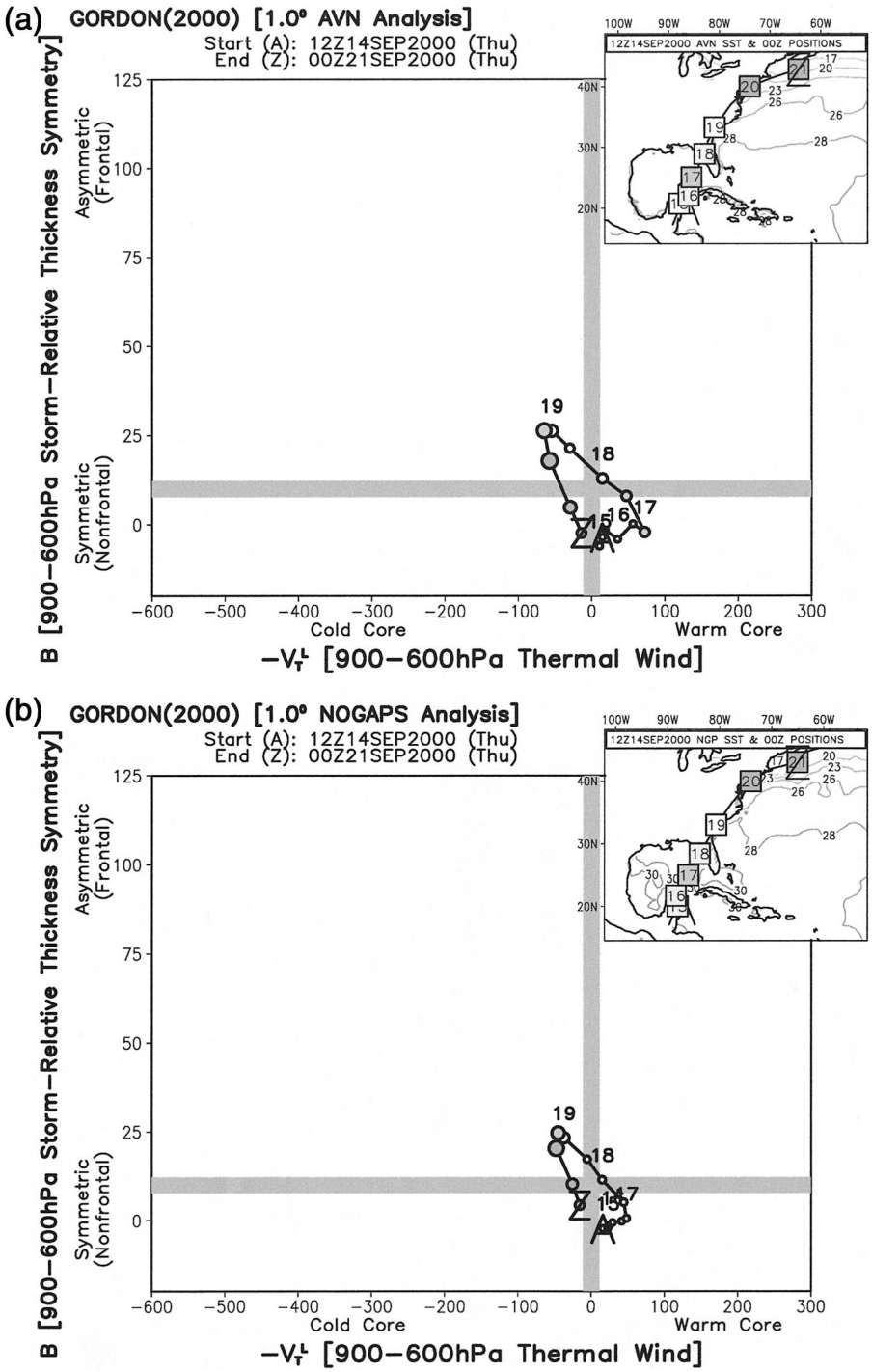

FIG. 11. Phase space diagnostic for Hurricane Gordon (2000) using (a) 1° AVN analyses and (b) 1° NOGAPS analyses. Symbols are as in Fig. 9.

gust for the Australian mainland of 267 km h^{-1} (74 m s^{-1}) recorded at the Learmonth Meteorological Office, shortly before 1200 LST on 21 March 1999 (see color images at the Bureau of Meteorology Website: http://www.bom.gov.au/info/cyclone/vancez.shtml). Typical of the ''captured'' transition class identified by Foley and Hanstrum (1994), Vance tracked rapidly southeastward, emerging into the Great Australian Bight at 1800 UTC on 23 March as it completed extratropical transition (Fig. 15). Vance reintensified as an extratropical cyclone for the following 24 h as it traversed eastward across the sub 20°C waters of the Great Australian Bight.

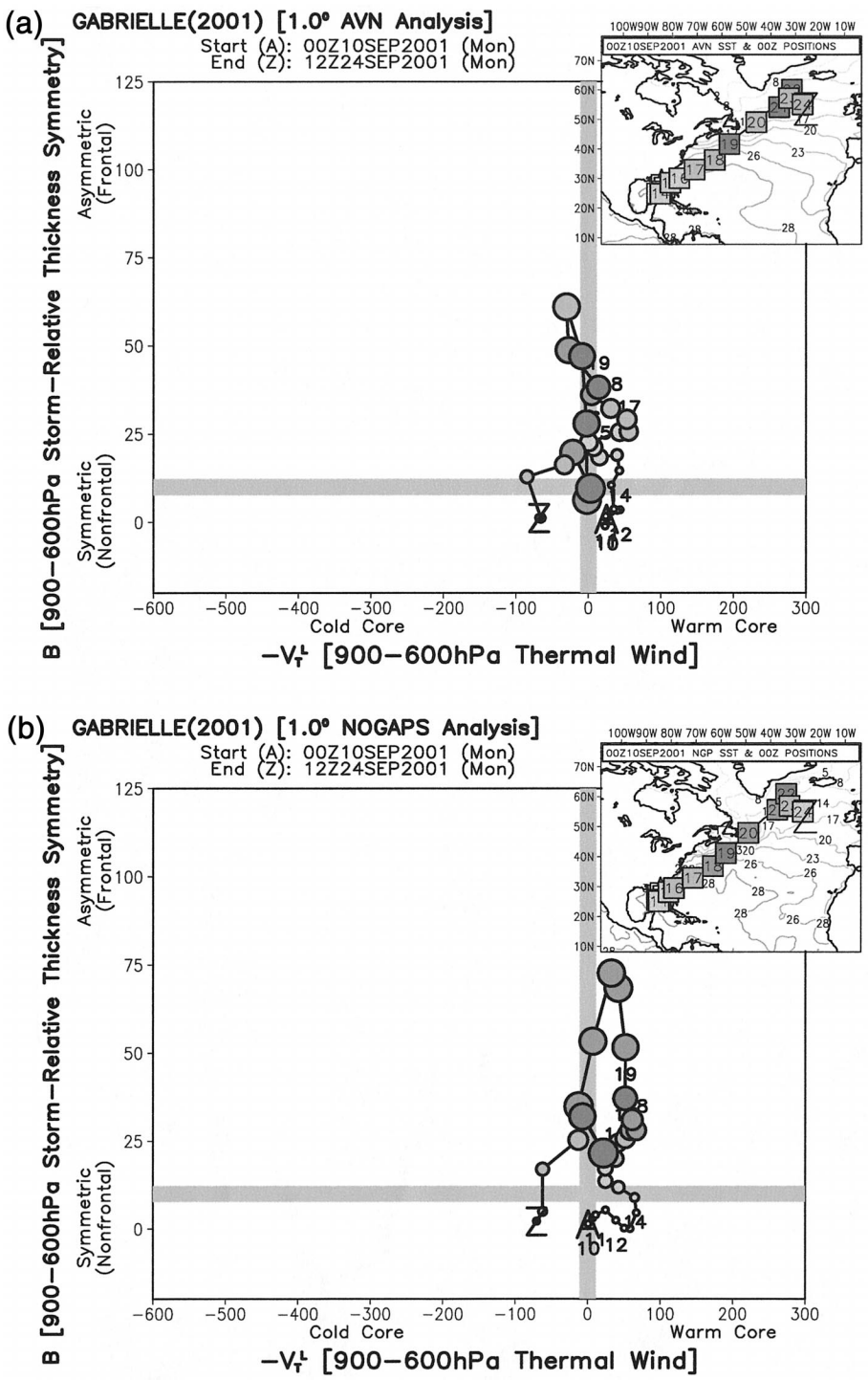

FIG. 12. Phase space diagnostic for Hurricane Gabrielle (2001) using (a) 1° AVN analyses and (b) 1° NOGAPS analyses. Symbols are as in Fig. 9.

6. Forecast issues and concluding summary

Objective definitions for the onset ($B > 10$ m) and completion ($-|\mathbf{V}_T^L| < 0$) of the extratropical transition of a tropical cyclone have been presented here. These definitions were developed using an initial set of 61 Atlantic cases from 1979 to 1993 and tested (section 5.2) on a set of 16 Atlantic cases from 1998 to 2001. The Australian case of Tropical Cyclone Vance (1999)

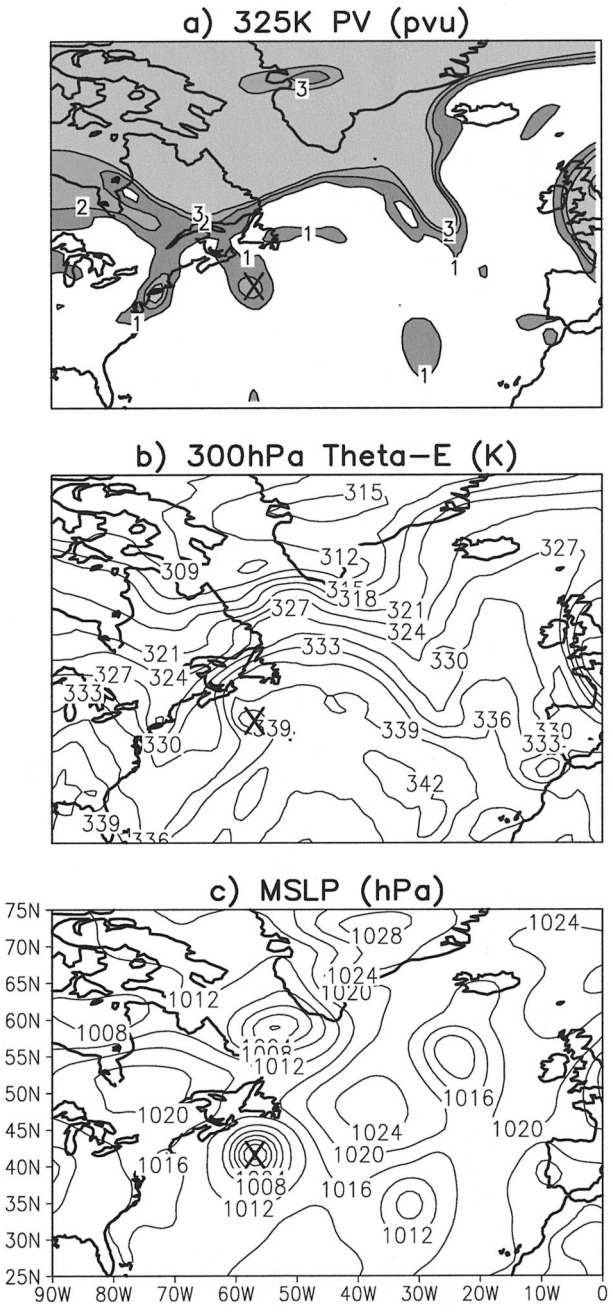

FIG. 13. AVN analyses of (a) 325-K potential vorticity, (b) 300-hPa equivalent potential temperature, and (c) mean sea level pressure for the Atlantic region at 0000 UTC 19 Sep 2001. Hurricane Gabrielle (2001) is in the process of extratropical transition at this time and is classified as a hybrid system using both the AVN and NOGAPS diagnostics (Fig. 12).

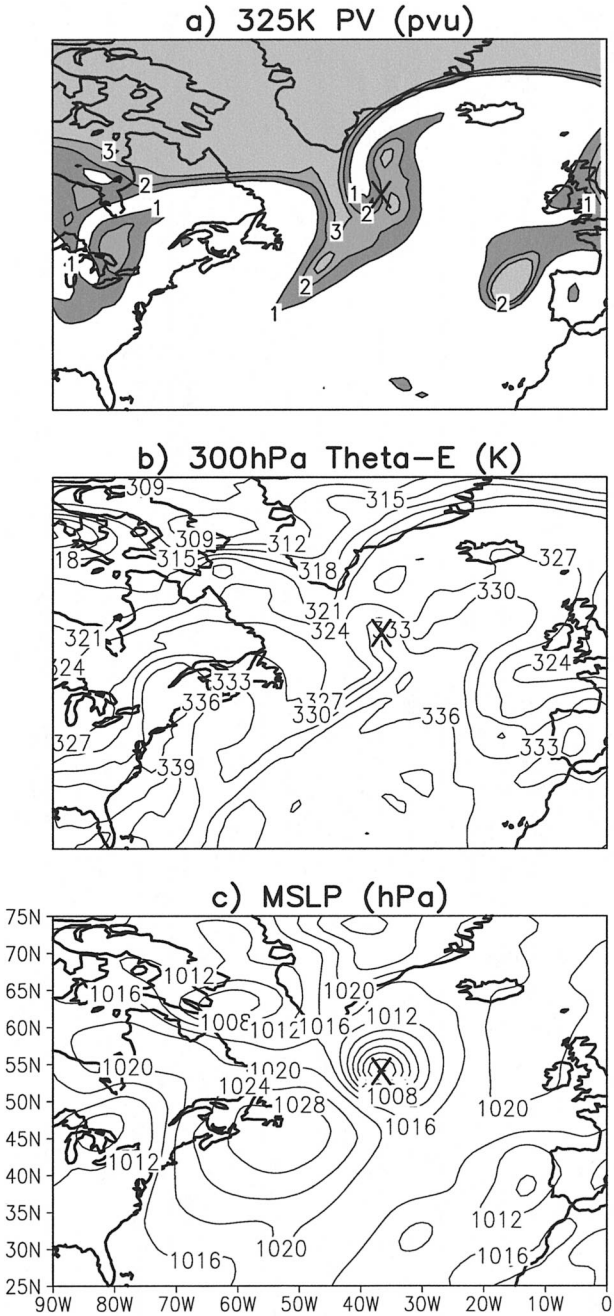

FIG. 14. AVN analyses of (a) 325-K potential vorticity, (b) 300-hPa equivalent potential temperature, and (c) mean sea level pressure for the Atlantic region at 0000 UTC 21 Sep 2001. Hurricane Gabrielle (2001) has completed extratropical transition at this time according to both the AVN and NOGAPS diagnostics (Fig. 12).

was also presented to demonstrate the wider applicability of these diagnostics across storm basins.

Timings of the NHC subjective declaration of extratropical transition for Atlantic storms and the objective ''completion'' diagnostic of cold-core development proposed here correspond reasonably well; however, there are some notable differences. The NHC best-track declaration time is compared to the objective declaration of extratropical transition in Table 1 for the 16-storm independent sample from 1998 to 2001. Objective transition data are derived from the AVN and NOGAPS operational analyses. The mean timing difference (MTD), absolute mean timing difference (AMTD), and

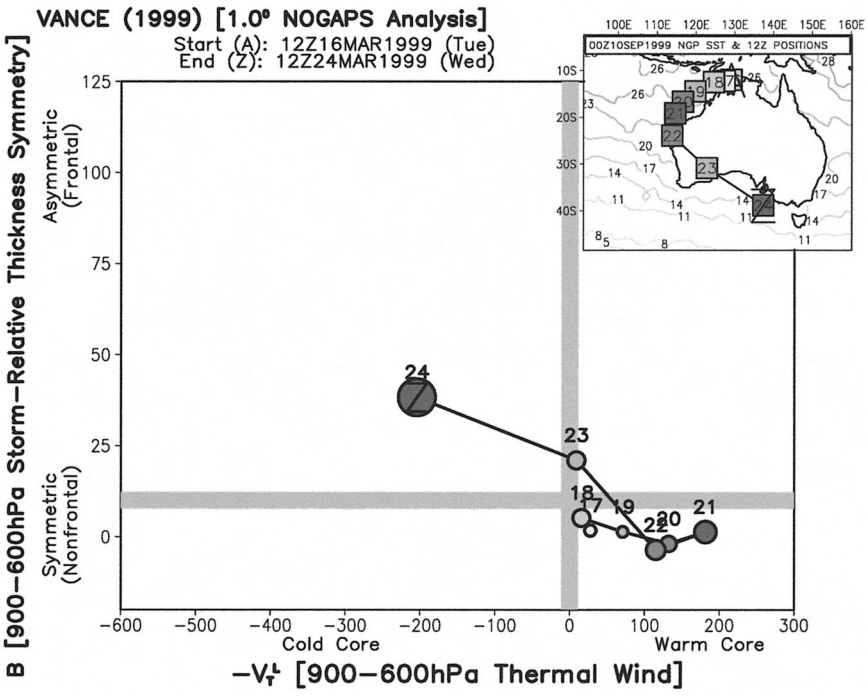

FIG. 15. Phase space diagnostic for Tropical Cyclone Vance (1999) in the South Indian Ocean. Diagnostics are calculated using the 1° NOGAPS analyses and symbols are as in Fig. 9, except that positions are labeled at 1200 UTC times (rather than 0000 UTC) since only 1200 UTC analyses were available. While this Australian tropical cyclone began as a tropical depression in the Coral Sea (east of the continent), only the period around transition (1200 UTC 16 Mar–1200 UTC 24 Mar 1999) is included here. The storm track and weekly averaged SST field are plotted in the inset. Wind gusts of 144 kt (an Australian record) were measured for Vance.

TABLE 1. Comparison of NHC best-track declaration of extratropical transition completion to the objective method for 16 cyclones from an independent dataset spanning 1998–2001. The time difference (in h) is given in the two rightmost columns for the two datasets used: 1° AVN and 1° NOGAPS operational analyses. The AVN incorporated a synthetic vortex from 1998 through 2000 and the NOGAPS incorporated a synthetic vortex for all 4 yr. In general, the NOGAPS synthetic vortex signature is more intense than the AVN for the 3 yr when both used the bogus. When gridded data were not available, or the vortex signature was too weak for reliable objective diagnosis, N/A is indicated. The last three rows indicate statistics for the extratropical transition diagnoses comparison: mean timing difference (MTD), absolute mean timing difference (AMTD), and standard deviation, respectively. For each model analysis, two numbers are given, seperated by a slash. The first number is the statistic for heterogeneous storm sample (12 storms for the AVN, 13 storms for the NOGAPS), while the second number is for the homogeneous storm sample (9 common storms between the two model analyses).

Year	Storm name	Date of NHC best-track declaration of extratropical transition	ET time offset of AVN phase diagnosis (h)	ET time offset of NOGAPS phase diagnosis (h)
1998	Bonnie	1800 UTC 30 Aug	N/A	−6
1998	Danielle	0000 UTC 4 Sep	N/A	+12
1998	Earl	1800 UTC 3 Sep	N/A	+18
1998	Mitch	1800 UTC 5 Nov	+6	+6
1999	Floyd	1200 UTC 17 Sep	0	+12
1999	Gert	1200 UTC 23 Sep	N/A	+24
2000	Alberto	1200 UTC 23 Aug	−12	−12
2000	Gordon	1800 UTC 18 Sep	−6	−6
2000	Michael	0000 UTC 20 Oct	+12	−12
2001	Allison	0000 UTC 18 Jun	0	−12
2001	Dean	1800 UTC 28 Aug	−18	N/A
2001	Erin	0600 UTC 15 Sep	+6	+6
2001	Gabrielle	0600 UTC 19 Sep	+6	+54
2001	Karen	1800 UTC 15 Oct	−18	N/A
2001	Michelle	0000 UTC 6 Nov	+12	+24
2001	Noel	1200 UTC 6 Nov	0	N/A
MTD			−1/+2.7	+8.3/+6.7
AMTD			+8/+6.7	+15.7/+16
σ			10.5/8	19.3/21.7

TABLE 2. Intercomparison of timing difference and absolute timing difference statistics for the years 1979–93 (41 cases; ECMWF 1.125° reanalyses) against the years 1998–2001. Three subsets of the most recent storm sample are documented: AVN and NOGAPS 1° operational analyses for the homogeneous sample of nine storms and the NOGAPS analyses for an eight-storm sample in which the major timing error of 54 h from Hurricane Gabrielle (1999) is removed. The mean and standard deviation of the actual timing difference and absolute timing difference are given as mean/std dev in all cases.

Years	No. of cases	Data source	Time difference (h)	Absolute time difference (h)
1979–93	41	ECMWF	−8.3/23.6	18.9/16.4
1998–2001	9	AVN	+2.7/8.0	6.7/4.7
	8	NOGAPS no Gabrielle	+0.8/13.4	11.3/5.9
	9	NOGAPS	+6.7/21.7	16/15.3

standard deviation of the NHC best-track transition declaration and objective transition are calculated. These statistics are presented for (i) all of the storm cases for which they are available in each model and (ii) only the homogeneous set of nine storms common to both models. These values are listed as (i)/(ii) for the MTD, MATD, and timing difference standard deviation in Table 1. From a quick scan of these results, one could conclude that the timing of transition in the AVN is in far better agreement with the NHC ET declaration than NOGAPS. However, if only the case of Hurricane Gabrielle (1999)—in which NOGAPS missed transition by 54 h—is removed, the NOGAPS timings of transition show more similar agreement with both NHC and AVN. This highlights the potential impact of a single poor analysis in the evaluation of model skill for a only few years.

Compared to the 61-storm sample from 1979 to 1993 (Fig. 7), there is a significant reduction in the magnitudes of the timing difference and absolute timing difference (both mean and standard deviation) for the AVN and NOGAPS (without Gabrielle) transition timings compared with NHC; the nine-case NOGAPS statistics are comparable with the earlier time period (Table 2). It is noteworthy that the mean timing difference has increased, from −8.3 in 1979–93 to between +2.7 and +6.7 in 1998–2001. This change represents a delay in the model transition time and is attributed to the more intense initial warm-core signatures present in the model analyses (compared to slightly coarser unbogused ECMWF reanalyses) during the tropical cyclone phase. The increase in intensity of the model tropical storm signature could be a result of the vortex bogusing and/or increases in model resolution. Such a result indicates that the intensity of the cyclone warm core has a direct impact upon the evolution and timing of extratropical transition. Further, the presence or absence of the tropical storm can affect the potential for extratropical cyclogenesis: for example, modeling studies with and without Hurricane Irene (1999) demonstrate that much weaker midlatitude cyclogenesis would likely have occurred without the hurricane (Prater-Mayer and Evans 2002).

The agreement between the objective phase space diagnosis and the NHC declaration of extratropical transition highlighted by this timing comparison suggests that the cyclone phase diagnoses described here capture the storm structure changes subjectively required by the operational forecasters. The objective ET criteria mapped in the cyclone phase space provide a repeatable diagnostic that can be used operationally to check the model consistency with the satellite signature and available observations of the storm. It is also useful as an aid for assessing improvements in model analysis and forecasting of tropical cyclones from tropical depression through extratropical transition and possibly in determining optimal timing for discontinuing storm bogusing in the analyses. Further, intercomparison of these diagnostics across model forecasts has the potential for evaluating storm forecast predictability.

Acknowledgments. Partial support for this research came from the National Science Foundation (ATM-9911212) and NASA (NAG5-7547). REM was funded by an Environmental Protection Agency (EPA) STAR Graduate Fellowship and a NASA Space Grant Graduate Fellowship. Sincere appreciation goes to these agencies for their support.

We thank Lixion Avila of NHC for his input on the methodology behind operational classification of transition at the U.S. National Hurricane Center. We further thank Mike Fiorino (LLNL) and Cdr. David Jones of NRL for providing access to the output from the operational NOGAPS. Analyses and figures for this paper were created using the GrADS software package. Satellite imagery provided by NCDC through their historical GOES browser at http://www.ncdc.gov/servlets/GoesBrowser.

REFERENCES

Atallah, E. H., 2001: The dynamics of heavy rainfall in landfallen tropical systems. Preprints, *First Symp. on Precipitation Extremes,* Albuquerque, NM, Amer. Meteor. Soc., 357–358.

Bosart, L. F., E. H. Atallah, and J. E. Molinari, 2001: The quantitative precipitation problem associated with landfalling and transitioning tropical cyclones. Preprints, *First Symp. on Precipitation Extremes,* Albuquerque, NM, Amer. Meteor. Soc., 359–362.

Bowyer, P., 2000: Phenomenal waves with a transitioning tropical cyclone (Luis, the Queen and the Buoys). Preprints, *24th Conf. on Hurricanes and Tropical Meteorology,* Fort Lauderdale, FL, Amer. Meteor. Soc., 294–295.

DiMego, G. J., and L. F. Bosart, 1982a: The transformation of Tropical Storm Agnes into an extratropical cyclone. Part I: The observed

fields and vertical motion computations. *Mon. Wea. Rev.*, **110,** 385–411.
——, and ——, 1982b: The transformation of Tropical Storm Agnes into an extratropical cyclone. Part II: Moisture, vorticity and kinetic energy budgets. *Mon. Wea. Rev.*, **110,** 412–433.
Elsberry, R. L., Ed., 1995: Global perspectives on tropical cyclones. WMO Tech. Doc. 693, Geneva, Switzerland, 289 pp.
Foley, G. R., and B. N. Hanstrum, 1994: The capture of tropical cyclones by cold fronts off the west coast of Australia. *Wea. Forcasting*, **9,** 577–592.
Frank, W. M., 1977a: The structure and energetics of the tropical cyclone. I. Storm structure. *Mon. Wea. Rev.*, **105,** 1119–1135.
——, 1977b: The structure and energetics of the tropical cyclone. II. Dynamics and energetics. *Mon. Wea. Rev.*, **105,** 1136–1150.
Gibson, J. K., P. Kållberg, S. Uppala, A. Hernandez, A. Nomura, and E. Serrano, 1997: ERA description. ECMWF Re-analysis Project Report Series, Part 1, ECMWF, Shinfield Park, Reading, United Kingdom.
Harr, P., and R. L. Elsberry, 2000: Extratropical transition of tropical cyclones over the western North Pacific. Part I: Evolution of structural characteristics during the transition process. *Mon. Wea. Rev.*, **128,** 2613–2633.
Hart, R. E., 1999: Working toward a conceptual model for extratropical transition: Diagnosis of transition and post-transition intensity change from observations and reanalyses. Preprints, *23d Conf. on Hurricanes and Tropical Meteorology*, Dallas, TX, Amer. Meteor. Soc. 805–808.
——, 2003: A cyclone phase space derived from thermal wind and thermal asymmetry. *Mon. Wea. Rev.*, **131,** 585–616.
——, and J. L. Evans, 2001: A climatology of extratropical transition of Atlantic tropical cyclones. *J. Climate*, **14,** 546–564.
Hirschberg, P. A., and J. M. Fritsch, 1993: On understanding height tendency. *Mon. Wea. Rev.*, **121,** 2646–2661.
Hogan, T., and T. Rosmond, 1991: The description of the Navy Operational Global Atmospheric Prediction System's spectral forecast model. *Mon. Wea. Rev.*, **119,** 1786–1815.
Kanamitsu, M., 1989: Description of the NMC global data assimilation and forecast system. *Wea. Forecasting*, **4,** 335–342.
Klein, P., P. Harr, and R. L. Elsberry, 2000: Extratropical transition of western North Pacific tropical cyclones: An overview and conceptual model of the transformation stage. *Wea. Forecasting*, **15,** 373–396.
Lawrence, M. B., L. A. Avila, J. L. Beven, J. L. Franklin, J. L. Guiney, and R. J. Pasch, 2001: Atlantic hurricane season of 1999. *Mon. Wea. Rev.*, **129,** 3057–3084.
MacAfee, A., and P. J. Bowyer, 2000a: Trapped fetch waves in a transitioning tropical cyclone (Part I—The need and the theory). Preprints, *24th Conf. on Hurricanes and Tropical Meteorology*, Fort Lauderdale, FL, Amer. Meteor. Soc., 292–293.
——, and ——, 2000b: Trapped fetch waves in a transitioning tropical cyclone (Part II—Analytical and predictive model). Preprints, *24th Conf. on Hurricanes and Tropical Meteorology*, Fort Lauderdale, FL, Amer. Meteor. Soc., 165–166.
Malmquist, D., 1999: Meteorologists and insurers explore extratropical transition of tropical cyclones. *Eos, Trans. Amer. Geophys. Union*, **80,** 79–80.
Molinari, J., and D. Vollaro, 1989: External influences on hurricane intensity. Part I: Outflow layer eddy angular momentum fluxes. *J. Atmos. Sci.*, **46,** 1093–1105.
——, and ——, 1990: External influences on hurricane intensity. Part II: Vertical structure and response of the hurricane vortex. *J. Atmos. Sci.*, **47,** 1902–1918.
Pasch, R. J., T. Kimberlain, and S. R. Stewart, 1999: Preliminary report on Hurricane Floyd 7–17 September 1999. National Hurricane Center, 27 pp. [Available from Tropical Prediction Center, 11691 S.W. 17th St., Miami, FL 33165-2149; also available online at http://www.nhc.noaa.gov/1999/floyd.html.]
Prater-Mayer, B., and J. L. Evans, 2002: Sensitivity of modeled tropical track and structure of Hurricane Irene (1999) to the convection parameterization scheme. *Meteor. Atmos. Phys.*, **80,** 103–115.
Reynolds, R. W., and T. Smith, 1995: A high-resolution global sea surface temperature climatology. *J. Climate*, **8,** 1571–1583.
Sekioka, M., 1956a: A hypothesis on complex of tropical and extratropical cyclones for typhoon in the middle latitudes. I. Synoptic structure of Typhoon Marie passing over the Japan Sea. *J. Meteor. Soc. Japan*, **34,** 276–287.
——, 1956b: A hypothesis on complex of tropical and extratropical cyclones for typhoon in the middle latitudes. II. Synoptic structure of Typhoons Louise, Kezia, and Jane passing over the Japan Sea. *J. Meteor. Soc. Japan*, **34,** 336–345.
Thorncroft, C., and S. C. Jones, 2000: The extratropical transition of Hurricanes Felix and Iris in 1995. *Mon. Wea. Rev.*, **128,** 947–972.